SSC-98

The Superconducting Super Collider

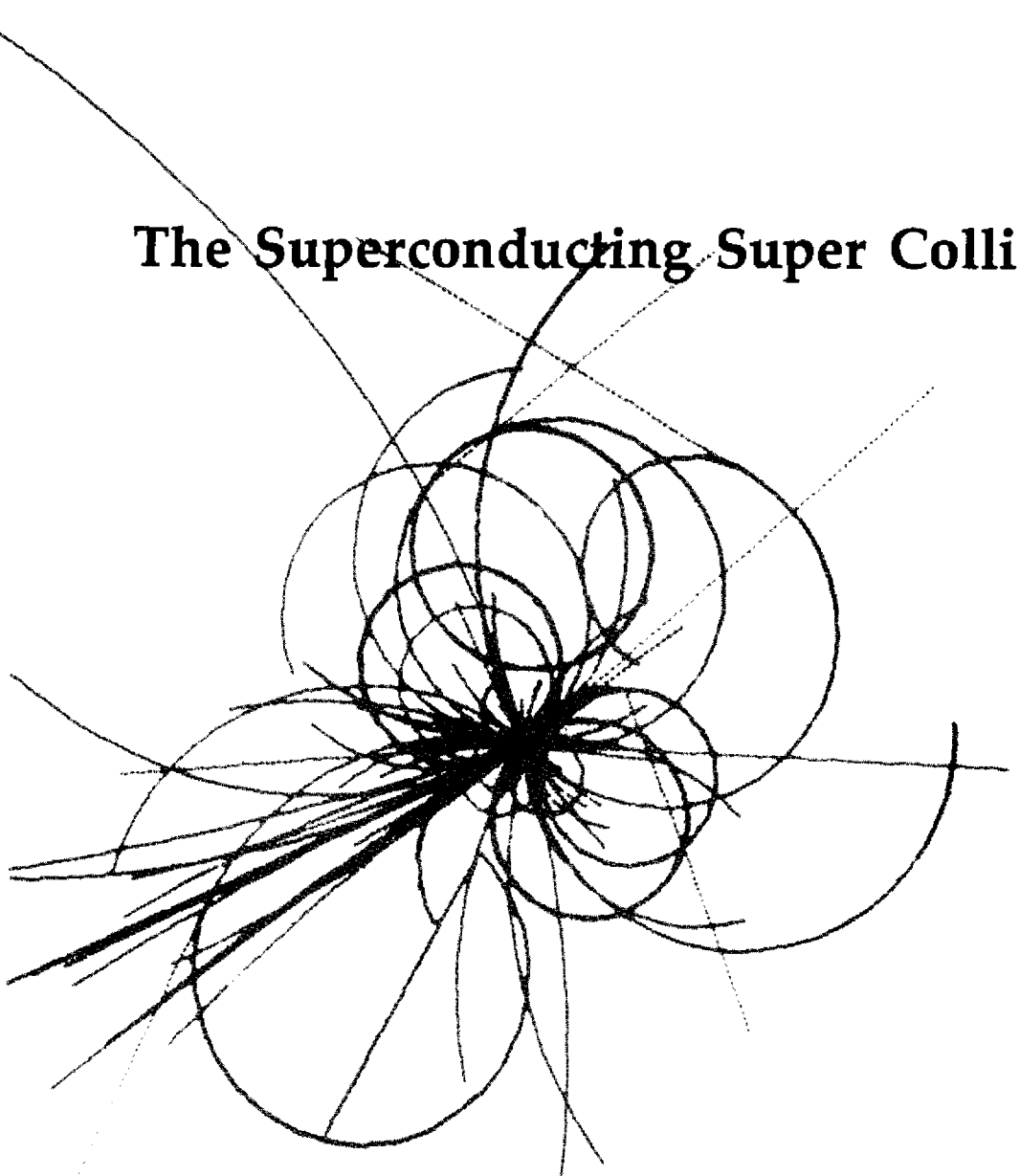

Dependence of Coherent Instabilities and Parasitic Heating on Vacuum Chamber Radius for the SSC

H. Lee and S. Chattopadhyay

SSC Central Design Group

September 1986

DEPENDENCE OF COHERENT INSTABILITIES AND PARASITIC HEATING ON VACUUM CHAMBER RADIUS FOR THE SSC*

H. Lee and S. Chattopadhyay
SSC Central Design Group
c/o Lawrence Berkeley Laboratory
Berkeley, California 94720

September 1986

*Operated by Universities Research Association, Inc. for the U. S. Department of Energy

DEPENDENCE OF COHERENT INSTABILITIES AND PARASITIC HEATING ON VACUUM CHAMBER RADIUS FOR THE SSC

Huan Lee and Swapan Chattopadhyay
SSC Central Design Group

September 1986

ABSTRACT

The impedance budget for SSC may have to be changed as a result of optimization of the cell lattice and aperture design. We have investigated the impact on the collective instabilities and parasitic heating if the vacuum chamber radius differs from the CDR value by as much as ±0.5 cm. We conclude that the corresponding changes on the cryogenic load due to parasitic heating are small, and most of the CDR conclusions on the collective instabilities remain intact. The requirements for the feedback gain and Landau damping to stabilize the transverse multibunch modes are modified somewhat, but can be met easily.

In this note we study the impact on collective instabilities and parasitic heating should the SSC vacuum chamber radius differ considerably from the value set in the conceptual design report[1] (CDR) as a result of cell lattice and aperture optimization. The growth rates, frequency shifts, and threshold criteria for various instabilities, as well as parasitic heating, all depend on the contributing impedances. As a first step, we examine systematically in the next section how different impedance sources scale with the vacuum chamber radius b. Effects on parasitic heating and instabilities are discussed in Secs. II and III. Conclusions are summarized in Sec. IV.

I. SCALING BEHAVIOR OF IMPEDANCE SOURCES

The total impedance in SSC consists of the contributions[1] from the following elements:

(a) rf cavities

(b) resistive wall of the vacuum chamber

(c) space charge

(d) beam position monitor pick-ups

(e) beam collimators

(f) bellows

(g) beam injection and abort kickers

(h) coherent synchrotron radiation

The impedance due to the beam collimators[1,2] is negligibly small compared with others, so it will not be considered here.

The impedances due to rf cavities and kickers do not change with b. Since we are mainly interested in the scaling behavior, we shall omit the explicit expressions for all the impedance sources to be discussed next. These expressions can be found in CDR.

Resistive Wall

Let $Z_{\parallel}(\omega)$ and $Z_{\perp}(\omega)$ be the longitudinal and transverse impedances corresponding to a radius b. The respective impedances used in CDR (with $b = b_0 \equiv 1.65$cm) are denoted by $Z^0_{\parallel}(\omega)$ and $Z^0_{\perp}(\omega)$. For resistive wall, we have

$$Z_{\parallel} = Z^0_{\parallel}(b_0/b) \tag{1}$$

$$Z_{\perp} = Z^0_{\perp}(b_0/b)^3 \tag{2}$$

Space Charge

For low frequency ($\omega \ll \gamma\, c/b$, where γ is the Lorentz factor for the beam), the longitudinal impedance for a round beam of radius a inside a perfectly conducting pipe behaves like

$$Z_{\parallel} = Z^0_{\parallel}\,[1+2\ln(b/a)]/[1+2\ln(b_0/a)] \tag{3}$$

Using $a = 4.5 \times 10^{-2}$cm at 1 TeV and $a = 1.0 \times 10^{-2}$cm at 20 TeV, $Z_{\parallel}$ changes ±7.5% and ±6%, respectively, for $b - b_0 = \pm 0.5$ cm. For our purpose, we can practically consider $Z_{\parallel}$ to be independent of b.

The transverse impedance scales like

$$Z_{\perp} = Z^0_{\perp}\,(a^{-2} - b^{-2})/(a^{-2} - b_0^{-2}) \tag{4}$$

Since $b \gg a$, again we can neglect the dependence of $Z_{\perp}$ on b.

Beam Position Monitors

For this item, we assume that the monitor length and the angle subtended by the strip electrodes remain unchanged, then the impedances scale as

$$Z_{\parallel} = Z_{\parallel}^{0} \tag{5}$$

$$Z_{\perp} = Z_{\perp}^{0}(b_0/b)^2 \tag{6}$$

Bellows

There is no simple formula to compute the impedance for bellows. In general, we have to recalculate each different geometry by computer code. However, scaling is possible if we assume either the bellows structure changes in proportion to b, or use the fact that the sliding contact shields form a shallow cavity with its length much greater than b.

1. Inner Bellows

We assume that the geometry of a single corrugation unit of the bellows scales similarly in proportion to b. The scaling behavior of the impedance can be obtained[3] by applying the scaling transformation in space and time to the Maxwell's equations. The results can be summarized as

$$Z_{\parallel}(\omega) = \frac{1}{\lambda} Z_{\parallel}^{0}(\lambda\omega) \tag{7}$$

$$Z_{\perp}(\omega) = (\frac{1}{\lambda})^2 Z_{\perp}^{0}(\lambda\omega) \tag{8}$$

where $\lambda = b/b_0$, and $Z(\omega)$ and $Z^0(\omega)$ are the total impedances for a fixed length. We stress that the impedance function changes not just by a multiplicative factor, but also scales in frequency spectrum.

2. Bellows with Sliding Contact Shields

As indicated in the diagram depicted in Fig. 4.5-4(a) of the CDR, we use g and Δ to denote the longitudinal and radial gaps, respectively, between the two sliding contact shields. It was pointed out in CDR that the impedance in this case consists of two parts; for convenience we call them resonant and non-resonant contributions. The resonant part comes from the cavity formed by sealing off the radial gap. The non-resonant part comes from the gap itself, which can be considered as a transmission line with inner and outer radii b and $(b + \Delta)$.

Since $b \gg \Delta$ and $b_0 \gg \Delta$, $Z_{\parallel}$ for the non-resonant part is simply

$$Z_{\parallel} = Z_{\parallel}^{0}\,[\ln(1+\Delta/b)]/[\ln(1+\Delta/b_0)] \approx Z_{\parallel}^{0}(b_0/b) \tag{9}$$

For $g \gg b$, which is valid in our case, it has been discussed[4] by Ng that the low frequency spectrum of the resonant part should also scale approximately in the same way.

For the transverse wake field, Bane and Ruth have demonstrated[5] numerically by using the computer code TBCI that the peak wake scales like

$$W_{\perp} = W_{\perp}^{0}(b_0/b)^3 \tag{10}$$

It follows that $\mathrm{Im}(Z_{\perp}(0))$ should also scale in the same manner. Since $Z_{\perp}$ is dominated by its imaginary part at low frequency, we can write approximately

$$|Z_{\perp}| \approx \mathrm{Im}Z_{\perp} \approx \mathrm{Im}Z_{\perp}^{0}(b_0/b)^3 \tag{11}$$

Coherent Synchrotron Radiation

This effect only contributes to the longitudinal impedance, and is proportional to b, so

$$Z_{\parallel} = Z_{\parallel}^{0} \, (b/b_0) \tag{12}$$

Now that the scaling behaviors for all impedance sources have been listed, we can readily estimate how the collective instabilities and parasitic heating are affected by changing the pipe radius. We first discuss the parasitic heating.

II. PARASITIC HEATING

In CDR, the parasitic heating power is computed by using a single-bunch formula

$$P = 2M(N_B e\omega_0/2\pi)^2 \sum_{p=0}^{\infty} \mathrm{Re}[Z_{\parallel}(p\omega_0)]\exp[-(p\omega_0\sigma_z/c)^2] \tag{13}$$

where M is the number of bunches per beam, N_B the number of particles per bunch, ω_0 the angular revolution frequency, and σ_z the rms longitudinal bunch spread. It has been pointed out recently that[6], while Eq. (13) is adequate for broad-band impedances, it is not so for impedances having sharp resonances, such as from rf cavities, due to the fact that M is very large for the SSC. The formula applicable to M equally spaced identical bunches is given by[5]

$$P = 2M^2(N_B e\omega_0/2\pi)^2 \sum_{p=0}^{\infty} \mathrm{Re}[Z_{\parallel}(p\omega_B)]\exp[-(p\omega_B\sigma_z/c)^2] \tag{14}$$

where $\omega_B = M\omega_0$.

In CDR, the rf cavity modes are computed based on the 358 MHz PEP parameter, rather than 374.7 MHz as chosen in the CDR. Since the bunch frequency ω_B for the SSC is rather high (62.5 MHz), the loss power calculated from Eq. (14) is quite sensitive to the cavity resonance frequencies. Therefore, it serves no useful purpose at this stage to recalculate the loss power due to rf cavities, before their design is fine-tuned to avoid the resonance frequencies being close to the multiples of ω_B. In any case, the parasitic loss for cavities fine-tuned in this way would be smaller than the value given in the CDR, which is computed from Eq. (13) rather than (14).

Since only the real part of $Z_{\parallel}$ contributes to P, the space change does not give rise to any parasitic loss. For all the impedance sources which scale by a multiplicative factor, the corresponding loss power scale in the same way.

For the inner bellows, its loss power cannot be scaled in a simple manner since the frequency spectrum of $Z_{\parallel}(\omega)$ also changes with b, as indicated in Eq.(7). Let us designate the right hand side of Eq.(13) by $P(b,\sigma_z)$ to show its functional dependence. Since we are dealing with a broad-band impedance here, the discrete sum over p in Eq.(13) can be approximated by an integral. With the scaling property in Eq.(7) it is easy to show that

$$P(b,\sigma_z) = (b_0/b)^2 P(b_0, b_0\sigma_z/b) \tag{15}$$

The plot $P(b_0,\sigma)$ vs σ has been computed by Furman[7] previously; using Eq.(15) we obtain $P(b,\sigma_z)$ easily.

In Table I we list the parasitic heating for various impedance sources in the cryogenic region. Notice that we use σ_z = 7.3 cm for consistency; whereas the values quoted in CDR are based on σ_z = 7 cm. We include the inner bellows for future reference, even though bellows with sliding contact shields are recommended by CDR. The subtotal does not include the inner bellows. The parasitic heating (from both beams) which contributes to the cryogenic load scales with b as

$$P = 0.32 + 0.524(b_0/b) \qquad \text{(in kW)} \tag{16}$$

Even for b = 1.15 cm, the cryogenic load due to parasitic heating is less than 1.1 kW, a modest 25% increase over the nominal CDR value.

The rf cavities and kickers are located in the room temperature sections; their parasitic loss power per beam are 270W and 220W, respectively, independent of b.

III. COLLECTIVE INSTABILITIES

Single Bunch Instabilities

For SSC, it is the mode-coupling (i.e. fast head-tail) instability that has the lowest threshold for transverse single bunch instability. This instability is driven by the low frequency imaginary part of the transverse impedance $Z_\perp$ (which leads to coherent frequency shifts of synchrotron modes, ultimately merging two mode frequencies, which determines the onset of the instability). The threshold value for the reactive part of $Z_\perp$ for the onset of transverse mode-coupling instability in the SSC bunch configuration is $Im(Z_\perp) = 250$ MΩ/m, at the injection energy of 1 TeV. For the same beam parameters, the threshold is twenty times higher at 20 TeV due to beam rigidity. In SSC, the beam parameters are different at 20 TeV from 1 TeV, but the threshold is still considerably higher at the higher energy.

In Table II, we have listed the dominant contributions to the low frequency reactive part of the transverse impedance $Z_\perp$ as a function of the beam pipe radius, using the scaling laws described before. The contributions from the rf cavities, beam collimators, and shielded coherent synchrotron radiation are negligible. The total reactive component $\Sigma|Im(Z_\perp)|$ ranges from 32 MΩ/m to 64 MΩ/m, as the beam pipe radius b is varied from 2.15 cm to 1.15 cm. These values are still way below the threshold (= 250 MΩ/m) for single bunch transverse mode-coupling instability. We conclude that the impact of varying the vacuum chamber radius as above on single bunch transverse instability for the SSC is benign.

In Table III, we have listed the dominant contributions to the low frequency $|Z_\parallel/n|$ for the longitudinal impedance, as a function of the beam pipe radius b, using the scaling laws described before. It ranges from .19 Ω to

.21 Ω as b varies from 2.15 cm to 1.15 cm. The threshold for longitudinal microwave instability at 1 TeV is $|Z_{\parallel}/n| = 15.5\ \Omega$, as calculated in the CDR. This threshold is far above the values .19 - .21 Ω envisaged for the SSC. Consequently, changing the vacuum chamber size has negligible effect on the longitudinal single bunch microwave instability.

Multibunch Instabilities

As noted in the CDR, the growth rates of the coupled bunch longitudinal and transverse instabilities are almost exclusively determined by the higher order parasitic modes of the rf cavity cells. Since this mode structure (both in strength and in frequency distribution) is relatively insensitive to the size of the vacuum chamber fitting into the rf cavity noses, the growth rates of the coupled bunch modes are almost unaffected by the vacuum chamber size scaling as envisaged, and the CDR values remain intact.

One exception to the above is the transverse rigid-dipole coupled bunch mode due to resistive wall, driven by the low frequency resistive part of the vacuum chamber impedance. This impedance is sharply peaked at the origin as $\omega^{-1/2}$ ($\omega \equiv 2\pi f$ is the circular frequency) and its strength increases as b^{-3} for decreasing radius b. Accordingly, the growth rate is enhanced significantly for smaller values of vacuum chamber radius b and reduced likewise for larger values of b. For b ranging from 1.15 cm to 2.15 cm, the short growth times range from 2.8 msec to 18.8 msec, for tunes below an integer by 0.1 (i.e. $\Delta\nu = 0.1$ as in the CDR). The frequency space structure and the conclusion that a feedback system is required to damp this instability, as expressed in the CDR, still remain valid. However, the gain of the feedback loop required may have to be increased by a factor of three (8.5 ms/2.8 ms ≃ 3) for b = 1.15 cm, implying an order of magnitude (factor of nine) increase in the

required kicker power, all other feedback parameters remaining the same. Since the unstable multibunch mode has a slow wave form from bunch to bunch, the bandwidth of the feedback system (response time $\approx$ revolution period) is narrow. The increase in the rquired power is therefore not serious.

Although the growth rates of all multibunch instabilities (except the transverse dipole modes due to resistive wall at low frequency) remain the same, the real coherent frequency shifts due to the low frequency reactive part of the broadband impedance will be different, owing to the scaling of the latter with b. It would seemingly affect the Landau damping of these multibunch coherent modes. For the longitudinal coupled bunch instabilities, although the space-charge and bellows reactive impedances at low frequencies can differ significantly from the CDR values (±10% for space-charge and ±40-50% for bellows), the total reactive ($Z_{\parallel}/n$) changes by only about ±5%. Thus Landau damping conclusions are almost unaffected in the CDR, for the longitudinal case. This has also been verified by the computer code ZAP[8], using different ($Z_{\parallel}/n$) values corresponding to different b's. We conclude that changing the vacuum chamber size by ± 0.5 cm has insignificant effect on the on the longitudinal Landau damping for the SSC.

With the CDR values $b = b_0$ and the momentum spread $\delta \equiv \Delta p/p$ equal to 1.75×10^{-4}, the largest real frequency shift for all non-rigid transverse coupled bunch modes is found to be $\Delta\Omega = 2 \times 10^{-4}\ \omega_0$, with ω_0 being the revolution frequency. Since $\Delta\Omega$ is linearly dependent on $Z_{\perp}$, from Table II we expect that $\Delta\Omega$ increases by 50% for the worst case b = 1.15 cm. On the other hand, $\Delta\Omega$ is inversely proportional to the bunch length σ_z, while the synchrotron tune spread $\Delta\nu_s$ is proportional to σ_z^2. Since $\sigma_z \propto \delta$, so we have $\Delta\Omega \propto \delta^{-1}$ and $\Delta\nu_s \propto \delta^2$. Therefore, to insure Landau damping for larger $\Delta\Omega$, we can increase either $\Delta\nu_s$, or the betatron tune spread $\Delta\nu_\beta$, or both.

We can summarize the stability criterion for b = 1.15 cm as

$$\Delta\nu_\beta > \frac{3}{f} - f^2 \times 10^{-4} \tag{17}$$

where f is the ratio of the increased δ over its CDR value. For example, to insure that all non-rigid transverse modes be Landau damped, from Eq. (17) we need $\Delta\nu_\beta > 2 \times 10^{-4}$ for f = 1, or $\Delta\nu_\beta > 1.5 \times 10^{-4}$ for f = 1.1, or $\Delta\nu_\beta > 10^{-4}$ for f = 1.2. Incidentally, it has been suggested recently by Zotter[9] that an increase in δ by about 15% would provide Landau damping for all longitudinal coupled bunch modes.

Finally, the unstable rigid dipole modes will in any case need a feedback system, as concluded in CDR. Growth rates of these rigid dipole modes are determined by the rf cavity impedance, and therefore are unaffected by the variation of b.

IV. CONCLUSIONS

To summarize, the impact on parasitic heating and collective instabilities tends to be less favorable for smaller pipe radius b. For the range of radius variation under consideration, changes in parasitic heating are mild, and most of the CDR conclusions on instabilities remain unchanged. The requirements for the feedback gain and Landau damping to stabilize the transverse multi-bunch modes are modified somewhat, but can be met easily. Following are more specific main conclusions.

1. The parasitic loss (in kW) which contributes to the cryogenic regions scales with b like $[0.32 + 0.524\ (b_0/b)]$. Even for b = 1.15 cm, this loss power is 1.1 kW, a modest increase of 25% over the CDR value. The parasitic loss which contributes to the room temperature region is independent of b.

2. All the CDR conclusions on the single bunch collective instabilities remain intact.

3. The growth rates of all multibunch instabilities remain essentially the same, except for the transverse dipole type due to resistive wall at low frequency. As discussed in the CDR, we need a feedback system to damp this instability in any case. However, the gain of the feedback loop required may have to be increased by a factor of $(b_0/b)^3$, about 3 for b = 1.15 cm.

4. For all the non-rigid, transverse coupled bunch modes, the Landau damping can be preserved by either a modest increase (20%) in $\Delta p/p$, or a larger betatron tune $\sim 2 \times 10^{-4}$ (twice the CDR value), or a combined modification as described by Eq. (17), for the worst case b = 1.15 cm.

5. As in the CDR, the transverse rigid dipole multibunch modes need a feedback system.

6. The Landau damping conclusions in CDR remain intact for the longitudinal multibunch instabilities, as we change b by ±0.5 cm.

Table I

Parasitic Heating of Sources in Cryogenic Region

Impedance Source	Loss Power (watts/beam)				
b (cm) =	1.15	1.4	1.65	1.9	2.15
Resistive Wall	96	79	67	58	51
Bellows					
-- inner bellows	(37)	(52)	(58)	(64)	(71)
-- sliding contact					
resonant	22	18	15	13	12
non-resonant	258	212	180	156	138
Beam Position Monitors	154	154	154	154	154
Coherent Synchrotron Radiation	4	5	6	7	8
Subtotal	534	468	422	388	363

Table II

Low Frequency Reactive Parts of $Z_\perp$ (in MΩ/m) for Different Radii

b (cm) =	1.15	1.4	1.65	1.9	2.15
Space Charge $\propto \frac{1}{a^2} - \frac{1}{b^2}$	21	21	21	21	21
Sliding Contact Bellows with Fixed $\Delta \propto b^{-3}$	20	12	7	4.5	3.2
Kickers ~ constant	1.4	1.4	1.4	1.4	1.4
Beam Position Monitors $\propto b^{-2}$	22	15	11	8.3	6.5
Total Reactive $Z_\perp$	64	49	39	35	32

Table III

Low Frequency $|Z_{\parallel}/n|$ (in Ohms) for Different Radii

b (cm) =	1.15	1.65	2.15
Space Charge $\propto [1 + 2\,\ln(b/a)]$	1.26×10^{-3}	1.4×10^{-3}	1.5×10^{-3}
Sliding Contact Bellows with Fixed "Δ" $\propto \ln(1 + \Delta/b) \approx (\Delta/b)$	.062	.043	.033
Kickers	.0915	.0915	.0915
Beam Position Monitors	.06	.06	.06
Total $|Z_{\parallel}/n|$	.21	.2	.19

REFERENCES AND ENDNOTES

1. "Conceptual Design," SSC Central Design Group Report No. SSC-SR-2020 (1986).

2. H. Lee, SSC Central Design Group Internal Report No. SSC-N-146 (1986).

3. H. Lee and A. Chao, SSC Central Design Group Internal Report No. SSC-N-241 (1986).

4. K.Y. Ng, SSC Central Design Group Report No. SSC-SR-1017 (1985), p. 61.

5. K. Bane and R. Ruth, SSC Central Design Group Report No. SSC-SR-1017 (1985), p. 10.

6. M. Furman, H. Lee, and B. Zotter, SSC Central Design Group Report No. SSC-86 (1986).

7. M. Furman, SSC Central Design Group Internal Report No. SSC-N-143 (1986).

8. M. Zisman, S. Chattopadhyay, and J.J. Bisognano, Lawrence Berkeley Laboratory Report No. LBL-21270 (1986).

9. B. Zotter, SSC Central Design Group Internal Report No. SSC-N-230 (1986).